METTL3-mediated m6A methylation and its impact on OTUD1 expression in chronic obstructive pulmonary disease

JIAMENG GAO[1*], ZHEYI SHEN[2*], WEIBIN TIAN[1*], JUNYI XIA[1], WEIXIN CAO[3], ZHUORU CHEN[3], ZHIHUA WANG[4] and YAO SHEN[1]

[1]Department of Respiratory and Critical Care Medicine, Shanghai Pudong Hospital, Fudan University Pudong Medical Center, Shanghai 201399, P.R. China; [2]Department of Ultrasound Medicine, Shanghai Pudong Hospital, Fudan University Pudong Medical Center, Shanghai 201399, P.R. China; [3]College of Basic Medicine, Hebei Medical University, Shijiazhuang, Hebei 050017, P.R. China; [4]Department of Geriatric Medicine, Shanghai Pudong Hospital, Fudan University Pudong Medical Center, Shanghai 201399, P.R. China

Received January 21, 2025; Accepted March 26, 2025

DOI: 10.3892/mmr.2025.13571

Abstract. Chronic obstructive pulmonary disease (COPD) is characterized by persistent airflow limitation and chronic inflammation, often exacerbated by cigarette smoke exposure. Ovarian tumor protease domain-containing protein 1 (OTUD1), a deubiquitinase, has previously been identified as a negative regulator of inflammation through its suppression of NF-κB signaling. The present study explored the role of OTUD1 in COPD and the regulatory effects of N6-methyladenosine (m6A) methylation on OTUD1 expression. The expression of OTUD1 in COPD was analyzed using public datasets (GSE38974 and GSE69818). In addition, BEAS-2B cells were exposed to cigarette smoke extract (CSE) to investigate OTUD1 expression changes. OTUD1 overexpression and knockdown models were also constructed, and the levels of inflammation-related genes and proteins, inflammatory cytokines and cell pyroptosis were measured using reverse transcription-quantitative PCR, western blotting, ELISA and flow cytometry. The role of methyltransferase-like 3 (METTL3)-mediated m6A methylation in regulating OTUD1 was also examined. Notably, OTUD1 expression was significantly reduced in advanced COPD compared with that in the earlier stage. Furthermore, CSE exposure suppressed OTUD1 expression, which was associated with increased cell pyroptosis and elevated levels of the inflammatory cytokines IL-1β and IL-18. OTUD1 overexpression mitigated these effects, indicating its protective role against CSE-induced cellular damage. Furthermore, METTL3-mediated m6A methylation inhibited OTUD1 expression, with YTH m6A RNA binding protein 2 (YTHDF2) acting as the reader of this modification. Knockdown of METTL3 or YTHDF2 reduced m6A methylation and restored OTUD1 expression, highlighting a potential mechanism by which cigarette smoke suppresses OTUD1 through enhanced m6A methylation. In conclusion, OTUD1 may serve a protective role in COPD by inhibiting inflammation and reducing cell damage caused by cigarette smoke exposure. The suppression of OTUD1 through METTL3-mediated m6A methylation and YTHDF2 interaction represents a novel mechanism contributing to COPD pathogenesis, suggesting potential therapeutic targets for mitigating disease progression.

Correspondence to: Dr Zhihua Wang, Department of Geriatric Medicine, Shanghai Pudong Hospital, Fudan University Pudong Medical Center, 2800 Gongwei Road, Shanghai 201399, P.R. China
E-mail: zhihua202410@163.com

Dr Yao Shen, Department of Respiratory and Critical Care Medicine, Shanghai Pudong Hospital, Fudan University Pudong Medical Center, 2800 Gongwei Road, Shanghai 201399, P.R. China
E-mail: shenyao1976@126.com

*Contributed equally

Abbreviations: COPD, chronic obstructive pulmonary disease; OTUD1, ovarian tumor protease domain-containing protein 1; CSE, cigarette smoke extract; m6A, N6-methyladenosine; METTL3, methyltransferase-like 3; YTHDF2, YTH m6A RNA binding protein 2; RT-qPCR, reverse transcription-quantitative PCR; RIP, RNA immunoprecipitation; TAK1, transforming growth factor β-activated kinase 1; EMT, epithelial-mesenchymal transition; GSDMD-N, gasdermin D N-terminal domain; NLRP3, NLR family pyrin domain containing 3

Key words: OTUD1, COPD, METTL3-mediated m6A methylation, mechanism

Introduction

The Global Initiative for Chronic Obstructive Lung Disease defines chronic obstructive pulmonary disease (COPD) as 'a common, preventable and treatable disease characterized by persistent airflow limitation due to airway and/or alveolar abnormalities, typically caused by significant exposure to toxic particles or gases' (1). The main pathological features of COPD include chronic and abnormal inflammatory responses mediated by the NF-κB signaling cascade in the lungs (2) and epithelial-mesenchymal transition (EMT) (3). As the third leading cause of death worldwide (4), the global mortality rate of COPD remains high, especially with the growing global population and increasing life expectancy. Moreover, the COVID-19 pandemic has notably impacted the quality of

care and experience for patients with COPD (5). Some studies have shown significantly increased mortality in patients with COPD infected with COVID-19 (up to 32.2%) (5,6). Therefore, there is a need to explore timely diagnostic and therapeutic approaches for COPD.

COPD is often considered a smoking-induced disease, with smoking (including secondhand smoke) being the most notable risk factor. A total of ~1.5 million of the 3 million global deaths from COPD each year are attributed to smoking (7), and 8 million individuals die annually from smoking-related diseases (8). Other factors associated with COPD include air pollution (9), occupational exposure (10), environmental tobacco smoke (11), infections and low socioeconomic status (12). Patients with advanced COPD often succumb to severe respiratory distress and acute exacerbations. Current treatments, such as bronchodilators and anti-inflammatory drugs, focus on symptom relief and exacerbation management rather than targeting disease progression and mortality, with the underlying mechanisms of inflammation in COPD development and treatment remaining unclear (13). Thus, the exploration into COPD mechanisms and the development of novel therapies are crucial, with an urgent need to develop treatments targeting immune dysfunction and underlying inflammation to slow COPD progression.

Ovarian tumor protease (OTU) domain-containing protein 1 (OTUD1) is a member of the OTU subfamily of deubiquitinating enzymes with an N-terminal disordered alanine, proline, glycine-rich region, catalytic OTU domain and ubiquitin-interacting motif. OTUD1 can cleave various ubiquitin linkages and is involved in regulating multiple cellular functions (14). Studies have shown that OTUD1 inhibits the progression of non-small cell lung cancer by mediating KLF4 stabilization, and that the deubiquitinase OTUD1, upregulated by VE-822, inhibits the progression of lung adenocarcinoma *in vitro* and *in vivo* by deubiquitinating and stabilizing FHL1 (15,16), suggesting new potential targets for treating non-small cell lung cancer and lung adenocarcinoma. In recent years, increasing evidence has demonstrated that OTUD1 inhibits the NF-κB pathway, thereby negatively regulating inflammation and serving an important role in inflammatory diseases (17,18). Studies have shown that OTUD1 negatively regulates inflammatory responses by inhibiting the activation of transforming growth factor-β-activated kinase 1 (TAK1)-mediated MAPK and NF-κB signaling pathways, providing protection against sepsis-induced lung injury, which may be related to the ability of OTUD1 to deubiquitinate TIPE2 (14,19). Furthermore, OTUD1 specifically reverses K63-linked ubiquitination of RIPK1 and inhibits NEMO recruitment, suppressing RIPK1-mediated NF-κB activation and preventing intestinal inflammation (17). Studies have also shown that RIP2 mediates ischemic brain injury by promoting inflammatory responses, whereas OTUD1 improves post-ischemic brain injury by specifically cleaving K63 ubiquitination of RIP2 and inhibiting RIP2-induced NF-κB activation (18,20).

In the present study, bioinformatics analysis predicted the presence of N6-methyladenosine (m6A) methylation sites in the 3'UTR of OTUD1. Related literature has indicated that methyltransferase-like 3 (METTL3) can promote m6A methylation (21) and COPD progression, whereas METTL3 silencing can reduce OTUD1 mRNA m6A methylation, thereby enhancing OTUD1 protein expression (22). YTH m6A RNA binding protein 2 (YTHDF2), a member of the YT521-B homology domain family 2, is an m6A 'reader' that recognizes m6A modifications and triggers a series of downstream biological responses. Increasing evidence has indicated that YTHDF2 serves notable roles in various mechanisms across both cancerous and non-cancerous conditions in patients (23-25). Therefore, the present study aimed to investigate the role of OTUD1 in COPD pathogenesis and its regulation by METTL3-mediated m6A methylation. Specifically, the study aimed to characterize OTUD1 expression patterns in COPD progression using public datasets (GSE38974 and GSE69818) and cigarette smoke extract (CSE)-exposed BEAS-2B cells; elucidate the functional impact of OTUD1 on inflammation and pyroptosis through overexpression and knockdown models, with a focus on NF-κB signaling and inflammasome-related pathways; and delineate the mechanism by which METTL3-driven m6A methylation, in collaboration with the reader YTHDF2, suppresses OTUD1 expression under CSE exposure. The findings aim to uncover novel therapeutic targets for COPD by linking epigenetic regulation of OTUD1 to inflammatory dysregulation in smoke-induced lung injury.

Materials and methods

Cell culture. The normal human lung epithelial cell line, BEAS-2B, was obtained from The Cell Bank of Type Culture Collection of The Chinese Academy of Sciences. BEAS-2B cells were cultured in a cell incubator with 5% CO_2 at 37˚C using Dulbecco's Modified Eagle's medium (DMEM; cat. no. SH30243.01; Hyclone; Cytiva) supplemented with 10% fetal bovine serum (cat. no. 16000e044; Gibco; Thermo Fisher Scientific, Inc.). Additionally, to avoid bacterial contamination, 1% penicillin with streptomycin (Beijing Solarbio Science & Technology Co., Ltd.) was added to the DMEM and the medium was replaced every 2-3 days.

Cell transfection. Cells were transfected with plasmids using Lipofectamine™ 3000 (Invitrogen; Thermo Fisher Scientific, Inc.) according to the manufacturer's instructions. Briefly, cells were seeded at a density of $2x10^5$ cells/well in 6-well plates 24 h prior to transfection to reach 70-80% confluence at the time of transfection. The concentrations of small interfering (si)RNAs and the pcDNA3.1 plasmid (Invitrogen; Thermo Fisher Scientific, Inc.) expressing OTUD1 (NM_001145373.3, CDS: 384-1,892) used for transfection were 50 nM and 2 μg per well, respectively. The empty pcDNA3.1 vector was used as a negative control for OTUD1 overexpression (vector group). The siRNAs were synthesized by Shanghai GenePharma Co., Ltd. Transfection was performed at 37˚C in a humidified atmosphere with 5% CO_2. Following transfection for 12 h, the cells were incubated for 48 h before being subjected to subsequent experiments. The sequences were as follows: OTUD1 siRNA (siOTUD1)-1 sense, 5'-AUCAUAGUGUCC GUUACUGAG-3', antisense, 5'-CUCAGUAACGGACAC UAUGAU-3'; siOTUD1-2 sense, 5'-UUUUAGACAAGGAUA UGGCCA-3', antisense, 5'-UGGCCAUAUCCUUGUCUA AAA-3'; siOTUD1-3 sense, 5'-UUUGAAAGUGCUAUUACC CUG-3', antisense, 5'-CAGGGUAAUAGCACUUUCAAA-3';

METTL3 siRNA (siMETTL3)-1 sense, 5'-UCUAACUCAGGAUCUGUAGCU-3', antisense, 5'-AGCUACAGAUCCUGAGUUAGA-3'; siMETTL3-2 sense, 5'-UGUGUUUAUUGAUAAUUCGUC-3', antisense 5'-GACGAAUUAUCAAUAAACACA-3'; siYTHDF2-1 sense, 5'-UUAAUCCAUCCUUUUGAUGUA-3', antisense, 5'-UACAUCAAAAGGAUGGAUUAA-3'; siYTHDF2-2 sense, 5'-ACUUUUGGAACAUUGCUUGCA-3', antisense, 5'-UGCAAGCAAUGUUCCAAAAGU-3'; siRNA-negative control (siNC) sense, 5'-UUCUCAGAACGUGUCACAU-3', antisense: 5'-AUGUGACACGUUCUGAGAA-3'.

Preparation of CSE and cell treatment. The aim of the present study was to simulate the microenvironment of cigarette smoke exposure in cell culture. The CSE solution was prepared on the day of the experiment. First, commercial cigarettes (each containing 2.5 mg nicotine and 12 mg tar; purchased from Shanghai, China) were drawn into a flask containing 10 ml DMEM at a rate of 1 cigarette every 3 min using a vacuum pump. The pH of the CSE solution was adjusted to 7.4, and the OD (A320-A540) was maintained between 0.9 and 1.2. The CSE solution was then filtered through a 0.22-μm filter to remove bacteria and other microorganisms. This solution was considered to be 100% CSE and was further diluted with DMEM to a working concentration of 10% for subsequent experiments, which were performed within 1 h of preparation as needed. After transfection with siRNA, cells were treated with the prepared CSE solution to simulate the cell culture environment. The treatment was performed at 37˚C for 24 h. Pyrrolidine dithiocarbamate (PDTC; 10 μM; cat. no. 52202ES50; Shanghai Yeasen Biotechnology Co., Ltd.), an NF-κB inhibitor that inhibits IκB phosphorylation, blocks NF-κB translocation into the nucleus and reduces the expression of downstream cytokines (26), was used to treat siOTUD1-transfected human BEAS-2B cells at 1 h post-transfection for 24 h at 37˚C.

ELISA. Secreted IL-1β and IL-18 levels in the supernatant were determined by ELISA. The cultured cells were centrifuged at 1,000 x g for 20 min at 4˚C, and after removing the cell pellets, the secreted IL-1β and IL-18 levels in the supernatant were quantified using human IL-1β and IL-18 ELISA kits (cat. nos. EK101B and EK118; Hangzhou Lianke Biology Technology Co., Ltd.), according to the manufacturer's instructions. The concentration of IL-1β and IL-18 was detected at 450 nm using a microplate reader (Bio-Rad Laboratories, Inc.).

Pyroptosis assay. To detect cell *pyropt*osis, cultured cells (~1x10^6 cells) were resuspended in PBS. Subsequently, anti-active caspase-1 (1:1,000; cat. no. MA5-32137; Invitrogen; Thermo Fisher Scientific, Inc.) was added and incubated for 1 h at 25˚C. The cells were then washed with PBS three times to remove non-combined caspase-1, followed by incubation with 3 μM propidium iodide solution (cat. no. P3566; Invitrogen; Thermo Fisher Scientific, Inc.) at room temperature for 15 min in the dark. Cell pyroptosis was assessed by flow cytometry (NovoCyte D3000; Agilent Technologies, Inc.) and analyzed using FlowJo 10.8.1 software (BD Biosciences), and the rate of cell pyroptosis was calculated.

Reporter gene assay. The OTUD1 3'UTR sequence was cloned into the pGL3 vector (Promega Corporation). BEAS-2B cells were co-transfected with siNC, siMETTL3-1 or siMETTL3-2 and the pGL3-OTUD1 3'UTR luciferase reporter plasmid, using Lipofectamine 3000 as the transfection reagent. The cells were cultured in 5% CO_2 at 37˚C for 24 h. Subsequently, the cells were lysed with lysis buffer (cat. no. 89901; Invitrogen; Thermo Fisher Scientific, Inc.), and the luciferase activity was measured by adding the *Renilla*-Firefly Luciferase Dual Assay Kit (MedChemExpress) luciferase substrate to the cell lysates. The luminescence was detected using a luminometer, and the luciferase activity was normalized to *Renilla* luciferase activity to assess the effects of METTL3 knockdown on OTUD1 3'UTR-mediated reporter expression.

RNA immunoprecipitation (RIP) and methylated RNA immunoprecipitation (meRIP) assay. The RIP assay was performed using the Magna MeRIP™ m6A Kit (MilliporeSigma). To isolate RNA-protein complexes, cells were cultured until they reached 70-80% confluence. RNA-protein complexes were crosslinked by adding 1% formaldehyde for 10-15 min at room temperature, and then quenched with 125 mM glycine for 5-10 min at 4˚C and rinsed with cold PBS. The cells (1x10^7) were lysed with a lysis buffer containing protease, RNase and phosphatase inhibitors, and the cells were homogenized, as required. Then, the RNA-protein complexes were conjugated with antibodies (5 μg): Anti-YTHDF2 (cat. no. ab220163; Abcam) or anti-IgG (cat. no. ab172730; Abcam) at 4˚C for 1 h. After which, the agarose beads and 50 μl protein A/G were added and incubated at 4˚C for 1 h. The beads were subsequently rinsed with lysis buffer to remove unbound material, and RNA was extracted using TRIzol® (cat. no. 15596026CN; Invitrogen; Thermo Fisher Scientific, Inc.) and treated with DNase to remove DNA contamination. Finally, RNA was analyzed by reverse transcription-quantitative PCR (RT-qPCR).

For meRIP, the aforementioned RNA-protein complexes were conjugated with 5 μg anti-m6A antibody (cat. no. ab208577; Abcam) at 4˚C for 1 h. The other processes were the same as those performed for the RIP experiment.

Actinomycin D treatment. A stock solution of actinomycin D (1 mg/ml in DMSO; MedChemExpress) was prepared. The stock solution was diluted to the desired working concentration (5 μg/ml) in culture medium. For treatment, the diluted actinomycin D solution was added to the culture medium at the desired concentration. It was ensured that the final concentration of DMSO did not exceed 0.1%. Cells were treated with actinomycin D at 37˚C for 4 h. The treatment was applied after transfection to ensure that any potential effects of actinomycin D on transcription could be accurately assessed in the context of the transfected cells.

RT-qPCR. To quantify mRNA expression levels, RT-qPCR was performed. Briefly, total RNA was extracted using TRIzol reagent and quantified using a spectrophotometer. RNA was reverse-transcribed using the PrimeScript™ RT reagent kit (Takara Bio, Inc.) according to the manufacturer's protocol. The RT reaction was carried out using 1 μg RNA in a total volume of 20 μl, with the following reaction conditions: 37˚C

for 15 min, followed by 85˚C for 5 sec to deactivate the reverse transcriptase enzyme. qPCR was carried out using SYBR Green qPCR Master Mix (Thermo Fisher Scientific, Inc.) on a C1000 thermal cycler (Bio-Rad Laboratories, Inc.) with the following cycling conditions: Initial denaturation at 95˚C for 5 min; 40 cycles at 95˚C for 30 sec, annealing at 60˚C for 30 sec and extension at 72˚C for 30 sec; and a final extension step at 72˚C for 5 min to ensure complete amplification. The primers used in the present study were self-designed based on the target gene sequences retrieved from GenBank (https://www.ncbi.nlm.nih.gov/genbank/). Primer design was carried out using Primer3 (version 0.4.0) (https://bioinfo.ut.ee/primer3-0.4.0/) to ensure appropriate melting temperatures and specificity. Primer sequences were synthesized by Sangon Biotech Co., Ltd. The Cq value was defined as the number of cycles needed for the fluorescent signal in the reaction tube to reach the set threshold. The relative mRNA levels normalized to GAPDH were calculated using the $2^{-\Delta\Delta Cq}$ method (27). The primer sequences for RT-qPCR were designed as follows: GAPDH forward (F), 5'-CACCATCTTCCAGGAGCGAG-3', reverse (R), 5'-TGATGACCCTTTTGGCTCCC-3'; OTUD1 F, 5'-TTTGGCTCAGTTGGCTCAGT-3', R, 5'-CGCGTTTCCTTTGCACTTGA-3'; OTUD1 3'UTR F, 5'-CUUACACCCUGGGAAUAAUUG-3', R, 5'-GATTAAGGCATTACACCTAC-3'; METTL3 F, 5'-GTGATCGTAGCTGAGGTTCGT-3', R 5'-GGGTTGCACATTGTGTGGTC-3'; YTHDF2, F, 5'-CAGGCAAGGCCCAATAATGC-3', R, 5'-AAGTAGGGCATGGCTGTGTC-3'.

Western blotting. The total protein was extracted from BEAS-2B cells using RIPA buffer (Beijing Solarbio Science & Technology Co., Ltd.), and the BCA protein assay kit (cat. no. A55864; Thermo Fisher Scientific, Inc.) was used to determine the protein levels. Subsequently, the samples were boiled at 95˚C for 10 min and proteins (20-40 μg/lane) were separated by SDS-PAGE on 10% gels at a constant voltage (80 V) until the dye front reached the bottom of the gel. The separated proteins were then transferred to a 0.2-μm PVDF membrane. For transfer, a constant current of 400 mA was applied for 1 h at 4˚C to ensure efficient transfer of proteins. The membranes were then blocked with 5% non-fat milk in TBST (20 mM Tris-HCl, 150 mM NaCl, 0.1% Tween-20, pH 7.4) for 1 h at room temperature to prevent non-specific binding of antibodies, followed by incubation with the following primary antibodies: NF-κB p65 (1:1,000; cat. no. ab32536; Abcam), NF-κB phosphorylated (p-) p65 (1:1,000; cat. no. ab76302; Abcam), active caspase-1 p20 (1:1,000; cat. no. abs154965; Absin Bioscience, Inc.), gasdermin D N-terminal domain (GSDMD-N; 1:1,000; cat. no. ab215203; Abcam), NLR family pyrin domain containing 3 (NLRP3; 1:1,000; cat. no. ab283819; Abcam), METTL3 (1:1,000; cat. no. ab195352; Abcam), YTHDF2 (1:1,000; cat. no. ab220163; Abcam), OTUD1 (1:1,000; cat. no. 29921-1-AP; Proteintech Group, Inc.), and GAPDH (1:5,000; cat. no. 60004-1-Ig; Proteintech Group, Inc.) at 4˚C overnight with gentle agitation. The membrane was washed three times with TBST and then incubated with horseradish peroxidase-conjugated secondary antibodies (1:1,000; cat. nos. A0208 and A0216; Beyotime Institute of Biotechnology) diluted in TBST containing 2% BSA (cat. no. 9048-46-8; Absin Bioscience, Inc.) for 1 h at 25˚C. Finally, the expression levels of proteins were measured using a chemiluminescent imaging system (Tanon 5200; Tanon Science and Technology Co., Ltd.).

Methylation site prediction. The present study employed a bioinformatics pipeline to predict methylation sites in the OTUD1 gene. The full-length mRNA sequence of *Homo sapiens* OTUD1 (accession no. NM_001145373.3, including 5'-UTR, CDS and 3'-UTR regions) was retrieved from the NCBI database (https://www.ncbi.nlm.nih.gov/nuccore/NM_001145373.3). CpG island and methylation region analyses were performed using the MethPrimer platform (https://www.urogene.org/methprimer/), which integrates sequence features (CpG dinucleotide density and GC content; thresholds: Length >200 bp, GC content >50%, observed/expected CpG ratio >0.6) with a machine learning model (random forest algorithm) to identify potential methylation sites, supplemented by cross-species conservation annotations. The 'full prediction' mode was selected for whole-sequence scanning, with RNA secondary structure analysis disabled, and a confidence threshold >0.7. Bioinformatics analysis using the SRAMP prediction server predicted the presence of an m6A methylation modification site in the OTUD1 3'UTR (http://www.cuilab.cn/m6asiteapp/old), and the predicted sites were validated against conserved regions in the MethDB (http://www.methdb.net/) and MethBank (https://ngdc.cncb.ac.cn/methbank/) databases, and CpG island-gene domain correlations were visualized via the UCSC Genome Browser (https://genome.ucsc.edu/).

Statistical analysis. The relevant data from two datasets in the Gene Expression Omnibus database [GSE38974 (https://www.ncbi.nlm.nih.gov/geo/query/acc.cgi?acc=GSE38974) and GSE69818 (https://www.ncbi.nlm.nih.gov/geo/query/acc.cgi?acc=GSE69818)] were integrated for subsequent analyses of differences in gene expression. Each experiment was performed in triplicate and data are presented as the mean ± standard deviation of three independent biological replicates. Statistical analyses were conducted using GraphPad Prism 7.0 software (Dotmatics). To compare differences in mean values among multiple groups, one-way analysis of variance followed by Tukey's post hoc test was applied. For comparisons between two groups, an unpaired two-tailed Student's t-test was used. $P<0.05$ was considered to indicate a statistically significant difference.

Results

Cigarette smoke stimulation inhibits OTUD1 expression. Analysis of COPD datasets GSE38974 (28) and GSE69818 (29) revealed that the expression levels of the OTUD1 gene were lower in advanced COPD compared with those in early COPD (Fig. S1). Subsequently, OTUD1 expression was detected in BEAS-2B cells treated with 10% CSE for 0, 12, 24 and 48 h using western blotting and RT-qPCR. RT-qPCR and western blotting results indicated that 10% CSE stimulation inhibited the expression levels of OTUD1 (Fig. 1A-C), demonstrating that cigarette smoke stimulation can decrease OTUD1 gene expression in human BEAS-2B cells.

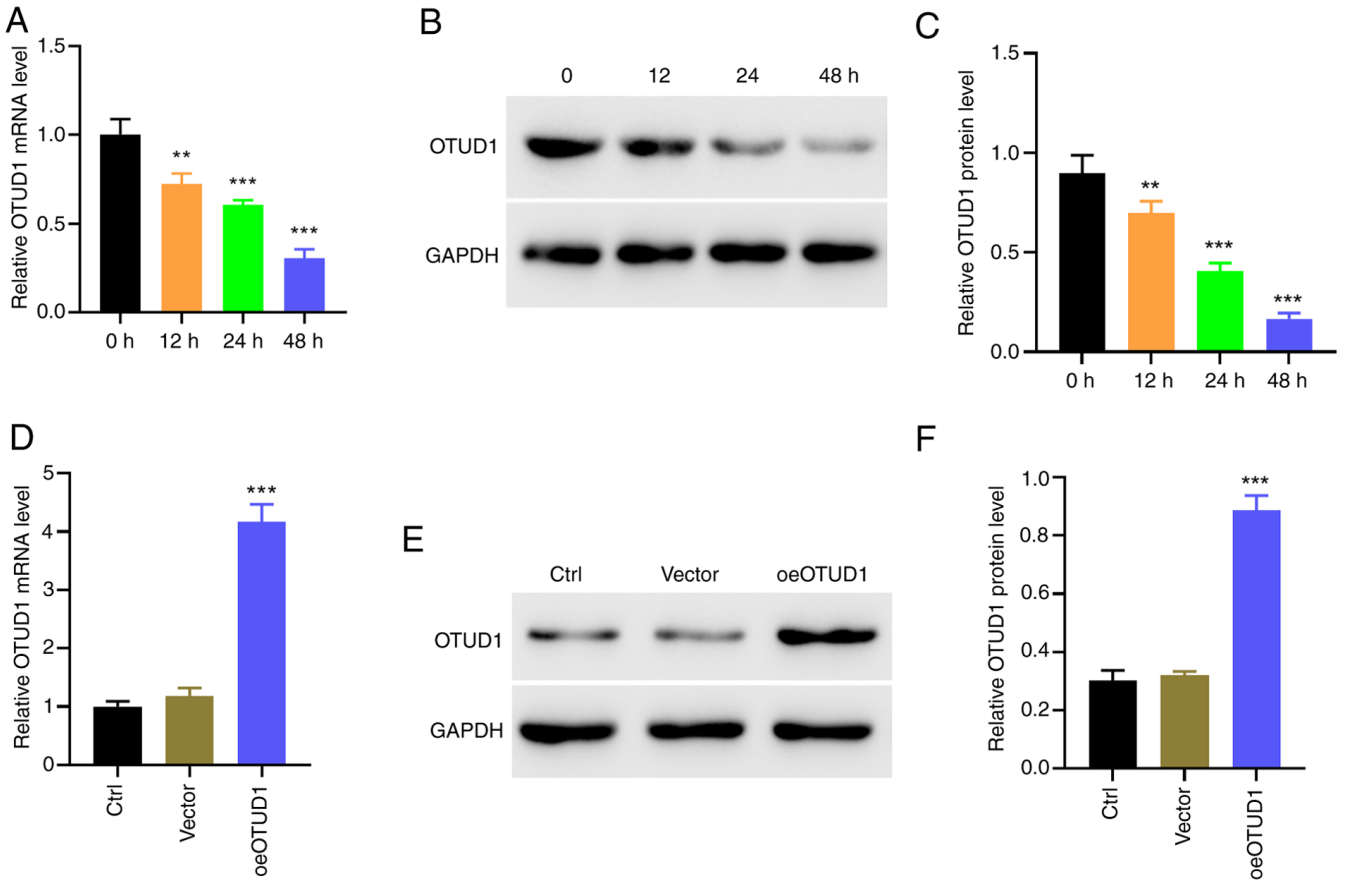

Figure 1. CSE (10%) inhibits OTUD1 mRNA and protein expression in BEAS-2B cells. BEAS-2B cells were treated with 10% CSE for 48 h. OTUD1 mRNA and protein expression levels were detected using (A) RT-qPCR and (B) western blotting at 0, 12, 24 and 48 h after intervention. (C) Semi-quantitative analysis of OTUD1 protein expression. **P<0.01, ***P<0.001 vs. 0 h. oeOTUD1 vectors were transfected into BEAS-2B cells for 24 h, and cytosolic OTUD1 mRNA and protein expression levels were detected using (D) RT-qPCR. (E) western blotting. (F) Semi-quantitative analysis of OTUD1 protein expression. ***P<0.001 vs. Vector. CSE, cigarette smoke extract; oe, overexpression; OTUD1, ovarian tumor protease domain-containing protein 1; RT-qPCR, reverse transcription-quantitative PCR.

OTUD1 reduces cellular damage caused by cigarette smoke stimulation by inhibiting the inflammatory response. To further verify that OTUD1 has a protective effect on cells stimulated with 10% CSE, an OTUD1 overexpression (oeOTUD1) plasmid was constructed and transfected into human BEAS-2B cells, after which, RT-qPCR and western blotting were used to verify the transfection efficiency of oeOTUD1 (Fig. 1D-F). Subsequently, human BEAS-2B cells were treated with 10% CSE, and pyroptosis was detected by flow cytometry (Fig. 2A and B). The results showed that pyroptosis was significantly increased in the 10% CSE-treated group compared with that in the vector group, whereas pyroptosis was reduced in the 10% CSE-treated oeOTUD1 group compared with that in the group treated with 10% CSE alone. To investigate whether the protective effect of OTUD1 on human BEAS-2B cells was related to inflammation, the levels of pro-inflammatory factors, NF-κB pathway proteins (p65 and p-p65) and proteins related to inflammasomes (NLRP3, p20 and GSDMD-N) were further detected. Common pro-inflammatory cytokines IL-1β and IL-18 were selected, and the levels of IL-1β and IL-18 in cell supernatants were detected by ELISA. The results showed that 10% CSE stimulation of human BEAS-2B cells resulted in a significant increase in IL-1β and IL-18 compared with that in normal human BEAS-2B cells; however, overexpression of OTUD1 could partially inhibit the elevation of IL-1β and IL-18 induced by cigarette smoke (Fig. 2C and D). To some extent, these findings verified that OTUD1 could serve a protective role in cells by reducing inflammation under cigarette smoke stimulation conditions. To further verify this hypothesis, NF-κB p65/NF-κB p-p65, NLRP3, active caspase-1 p20 and GSDMD-N were detected by western blotting. The results showed that the expression levels of NF-κB p65/NF-κB p-p65, NLRP3, active caspase-1,p20 and GSDMD-N were significantly increased in the cell group treated with 10% CSE, whereas they were reduced in the oeOTUD1 group (Fig. 2E-I). These findings further validated that OTUD1 expression may serve a protective role in cells by inhibiting inflammation.

Reverse validation of the protective effect of OTUD1 on cells through inhibition of the inflammatory response in BEAS-2B cells. In the present study, reverse validation was performed, whereby siOTUD1-transfected human BEAS-2B cells were constructed, and the transfection efficiency of siOTUD1 was verified by RT-qPCR and western blotting (Fig. 3A-C). The cells were divided into the following three siRNA groups: i) siOTUD1-1; ii) siOTUD1-2; and iii) siOTUD1-3. And the siOTUD1-1was used in subsequent experiments, as it induced lower OTUD1 protein levels. The results of the pyroptosis assay

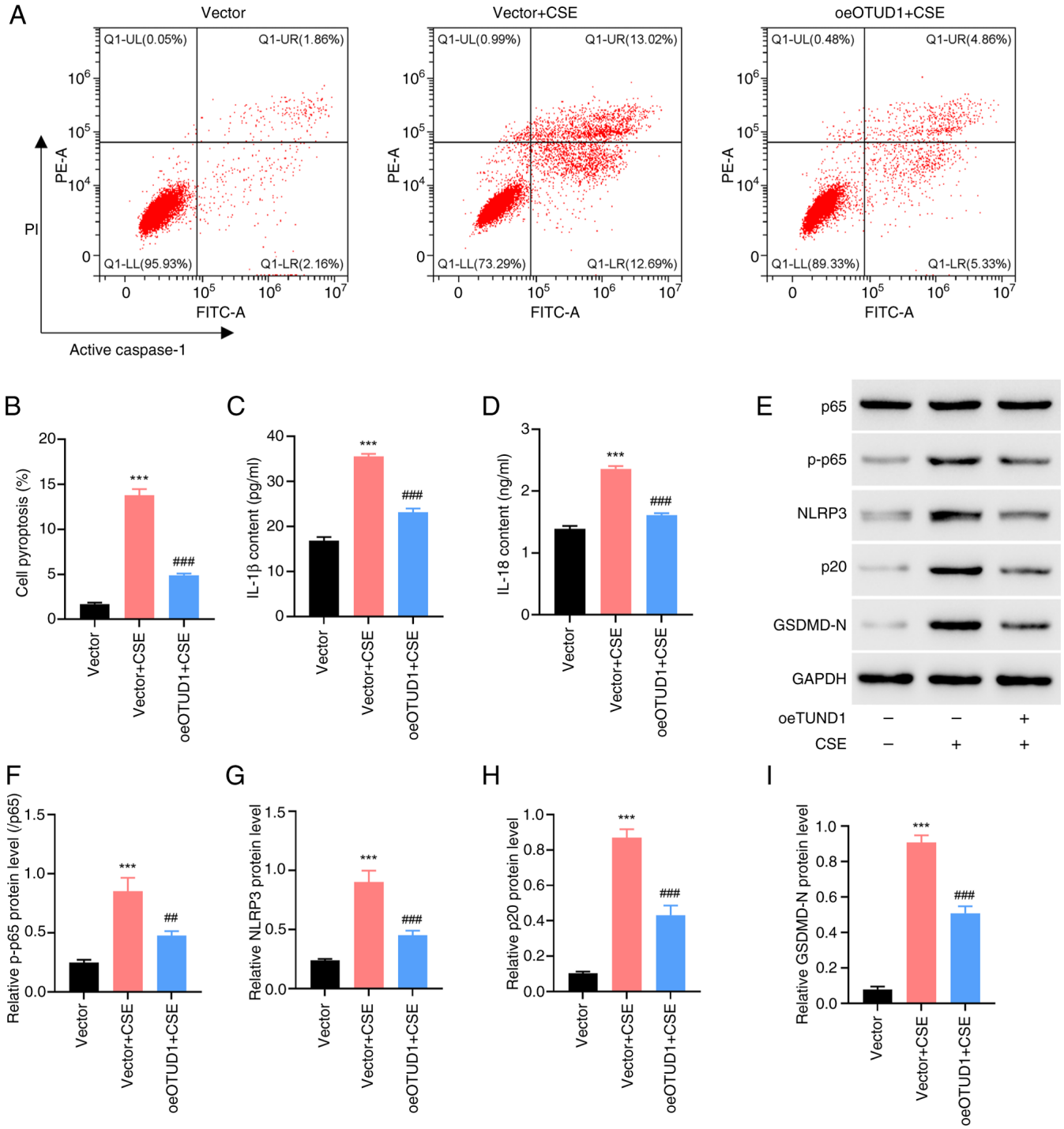

Figure 2. oeOTUD1 ameliorates 10% CSE-induced BEAS-2B cell pyroptosis. BEAS-2B cells were transfected with oeOTUD1 vector and treated with 10% CSE for 24 h. (A) Flow cytometry was performed to detect cell pyroptosis. (B) Quantitative analysis of cell pyroptosis. ELISA was performed to detect changes in (C) IL-1β and (D) IL-18 levels in the cell supernatants. (E) Western blot analysis was performed to detect the protein expression levels of (F) NF-κB p65 and NF-κB p-p65, (G) NLRP3, (H) active caspase-1 p20 and (I) GSDMD-N. ***P<0.001 vs. Vector; $^{\#\#}$P<0.01, $^{\#\#\#}$P<0.001 vs. Vector + CSE. Vector, empty pcDNA3.1 vector; CSE, cigarette smoke extract; GSDMD-N, gasdermin D N-terminal domain; NLRP3, NLR family pyrin domain containing 3; oe, overexpression; OTUD1, ovarian tumor protease domain-containing protein 1; p-, phosphorylated.

suggested that pyroptosis was significantly increased after knockdown of OTUD1, whereas the addition of the NF-κB inhibitor PDTC resulted in a decrease in pyroptosis compared with that in the siOTUD1 group (Fig. 3D and E). Subsequently, ELISA was performed to detect the levels of IL-1β and IL-18 in cell supernatants; the results were consistent with the pyroptosis assay results, after silencing the expression of OTUD1, the levels of the pro-inflammatory cytokines IL-1β and IL-18 were significantly increased, whereas this increase was inhibited by the addition of the NF-κB inhibitor PDTC (Fig. 3F and G). Furthermore, the expression levels of NF-κB p65/NF-κB p-p65, NLRP3, active caspase-1 p20 and GSDMD-N were examined by western blotting, and the results also showed that the expression of these proteins were markedly increased

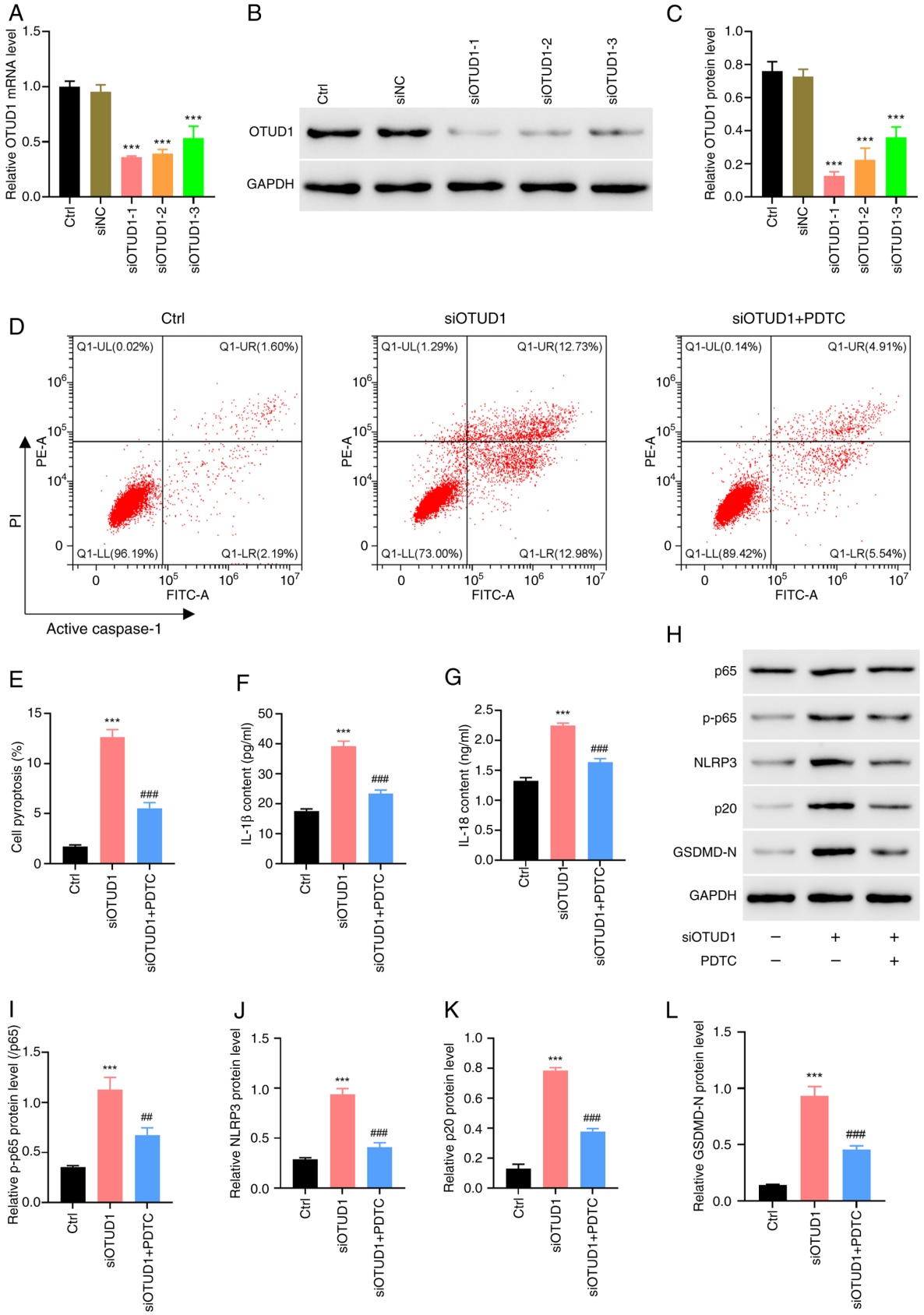

Figure 3. siOTUD1 induces BEAS-2B cell pyroptosis, which is inhibited by treatment with the NF-κB inhibitor PDTC. A total of 24 h after transfection of BEAS-2B cells with siOTUD1, changes in cytosolic mRNA and protein expression levels of OTUD1 were detected using (A) reverse transcription-quantitative PCR and (B) western blotting. (C) Semi-quantitative analysis of OTUD1 protein expression. siOTUD1-1 was used for subsequent experiments. BEAS-2B cells transfected with siOTUD1 were simultaneously co-treated with PDTC (100 μM) for 24 h. (D) Flow cytometry was performed to detect cell pyroptosis. (E) Quantitative analysis of cell pyroptosis. ELISA was performed to detect the changes in (F) IL-1β and (G) IL-18 levels in cell supernatants. (H) Western blotting was performed to detect the protein expression levels of (I) NF-κB p65 and NF-κB p-p65, (J) NLRP3, (K) active caspase-1 p20 and (L) GSDMD-N. ***P<0.001 vs. Ctrl; $^{\#\#}$P<0.01, $^{\#\#\#}$P<0.001 vs. siOTUD1. GSDMD-N, gasdermin D N-terminal domain; NC, negative control; NLRP3, NLR family pyrin domain containing 3; oe, overexpression; OTUD1, ovarian tumor protease domain-containing protein 1; p-, phosphorylated; si, small interfering.

after silencing the expression of OTUD1, whereas the NF-κB inhibitor PDTC could attenuate the elevated inflammatory response induced by OTUD1 knockdown (Fig. 3H-L). These findings indicated that OTUD1 could serve a protective role in patients with COPD and that this protective effect may be achieved through its anti-inflammatory effects.

CSE stimulation promotes OTUD1 methylation by increasing METTL3 activity, which in turn inhibits OTUD1 gene expression. Relevant studies have shown that METTL3 expression is significantly elevated in patients with smoking-induced COPD and COPD cell models, and that METTL3-mediated modification of m6A RNA methylation regulates CSE-induced EMT by targeting OTUD1 mRNA, ultimately serving a key regulatory role in the emergence of COPD (30-32). Bioinformatics analysis predicted the presence of an m6A methylation modification site in the OTUD1 3'UTR. meRIP-qPCR of OTUD1 methylation levels in human BEAS-2B cells treated with 10% CSE demonstrated that the m6A methylation level was significantly elevated in the 10% CSE-treated cells compared with that in the control group (Fig. 4A), which indicated that 10% CSE stimulation could inhibit OTUD1 expression by increasing m6A.

After human BEAS-2B cells were treated with 10% CSE, METTL3 expression was detected by RT-qPCR and western blotting; the results showed that the expression levels of METTL3 were elevated in the 10% CSE group (Fig. 4B-D). These findings indicated that cigarette smoke stimulation may increase m6A methylation through increasing METTL3 activity levels, which in turn inhibits the expression of OTUD1.

To provide further verification, 10% CSE-treated human BEAS-2B cells transfected with siMETTL3 underwent meRIP-qPCR to detect the m6A methylation level of OTUD1. RT-qPCR and western blotting were used to detect the expression levels of OTUD1, and a luciferase reporter gene was used to detect the 3'UTR activity of OTUD1. The results showed that the methylation level of OTUD1 was decreased, and the expression levels of OTUD1 and the 3'UTR activity of OTUD1 were increased in cells transfected with siMETTL3 and stimulated with 10% CSE compared with those in the group stimulated with 10% CSE alone (Fig. 4E-L). Therefore, by knocking down METTL3, it was further verified that 10% CSE stimulation may promote OTUD1 methylation by increasing METTL3 activity, which in turn suppresses OTUD1 gene expression. Since transfection with siMETTL3-1 resulted in the lowest METTL3 protein levels, siMETTL3-1 was used in the subsequent experiments.

Inhibition of the m6A methylation reader YTHDF2 mitigates the increased methylation of OTUD1 induced by 10% CSE. To assess the transfection efficiency of siYTHDF2, the expression levels of YTHDF2 were detected in human BEAS-2B cells transfected with siYTHDF2 using RT-qPCR and western blotting (Fig. 5A-C). siYTHDF2-1 was used in the subsequent experiments as it induced lower YTHDF2 protein levels than siYTHDF2-2. Actinomycin D, a transcription inhibitor, forms stable complexes by intercalating into DNA, blocking DNA-dependent RNA polymerase activity, and thereby inhibiting transcription, making it a common tool for RNA stability assays (16). BEAS-2B cells with YTHDF2 knockdown were treated with 10% CSE and 5 μg/ml actinomycin D for 0.5, 3 and 6 h, followed by RT-qPCR to assess OTUD1 transcription levels. The results showed that OTUD1 expression was higher in the group treated with 10% CSE combined with YTHDF2 knockdown compared with that in the group treated with 10% CSE alone (Fig. 5D), thus indicating that YTHDF2 inhibition also suppressed m6A methylation, thereby partially relieving the suppression of OTUD1 expression.

To validate this hypothesis, BEAS-2B cells were treated with 10% CSE, and meRIP-qPCR was performed to detect the binding of YTHDF2 to the 3'UTR of OTUD1. The results indicated that cigarette smoke exposure increased the binding of YTHDF2 to the OTUD1 3'UTR (Fig. 5E). Furthermore, in BEAS-2B cells treated with 10% CSE alone or combined with METTL3 knockdown, meRIP-qPCR was used to assess YTHDF2 binding to the OTUD1 3'UTR. The results showed that METTL3 inhibition reduced the binding of YTHDF2 to the OTUD1 3'UTR (Fig. 5F).

Discussion

Recent studies have shown that OTUD1 regulates the NF-κB pathway primarily by inhibition, inducing protective effects on sepsis-induced lung injury, inflammatory bowel disease and inflammation-mediated ischemic brain injury (17,18). Specifically, OTUD1 inhibits the activation of certain inflammatory pathways, such as the NF-κB pathway, by removing ubiquitin from key signaling proteins (33). This deubiquitination activity prevents the activation of NF-κB, which serves a central role in promoting inflammation. For example, in the NF-κB pathway, OTUD1 serves a role in preventing the activation of NF-κB by removing K63-linked ubiquitin chains from RIPK1. This de-ubiquitination process reduces the ability of NEMO (a key protein in the NF-κB signaling pathway) to bind to RIPK1, thus suppressing the activation of NF-κB signaling. Essentially, OTUD1 acts as a negative regulator of this pathway (34). In addition, OTUD1 inhibits TAK1-mediated MAPK and NF-κB pathways (35) to reduce inflammation in conditions such as sepsis-induced lung injury and ischemic brain injury. Furthermore, OTUD1 deubiquitinase regulates NF-κB- and KEAP1-mediated inflammatory and oxidative stress responses (34). Overall, OTUD1 acts as a negative regulator of these pathways by inhibiting their activation, which aids suppression of excessive inflammation. The anti-inflammatory effects of OTUD1 may indicate a novel role in COPD.

In the present study, the analysis of COPD datasets (GSE38974 and GSE69818) revealed that OTUD1 expression was lower in advanced COPD compared with that in the earlier stage. To assess the role of OTUD1 in COPD progression, BEAS-2B cells were stimulated with 10% CSE, and the results indicated that OTUD1 expression was decreased under CSE. To further confirm the role of OTUD1, oeOTUD1 models were constructed in BEAS-2B cells. Under similar CSE conditions, cells in the oeOTUD1 group exhibited reduced pyroptosis, decreased levels of the pro-inflammatory cytokines IL-1β and IL-18, and reduced expression levels of NF-κB and inflammasome-related proteins compared with those in the control group. These findings suggested that OTUD1 may reduce cell damage and pyroptosis induced by 10% CSE through inhibiting inflammation. To validate this further, siOTUD1 models

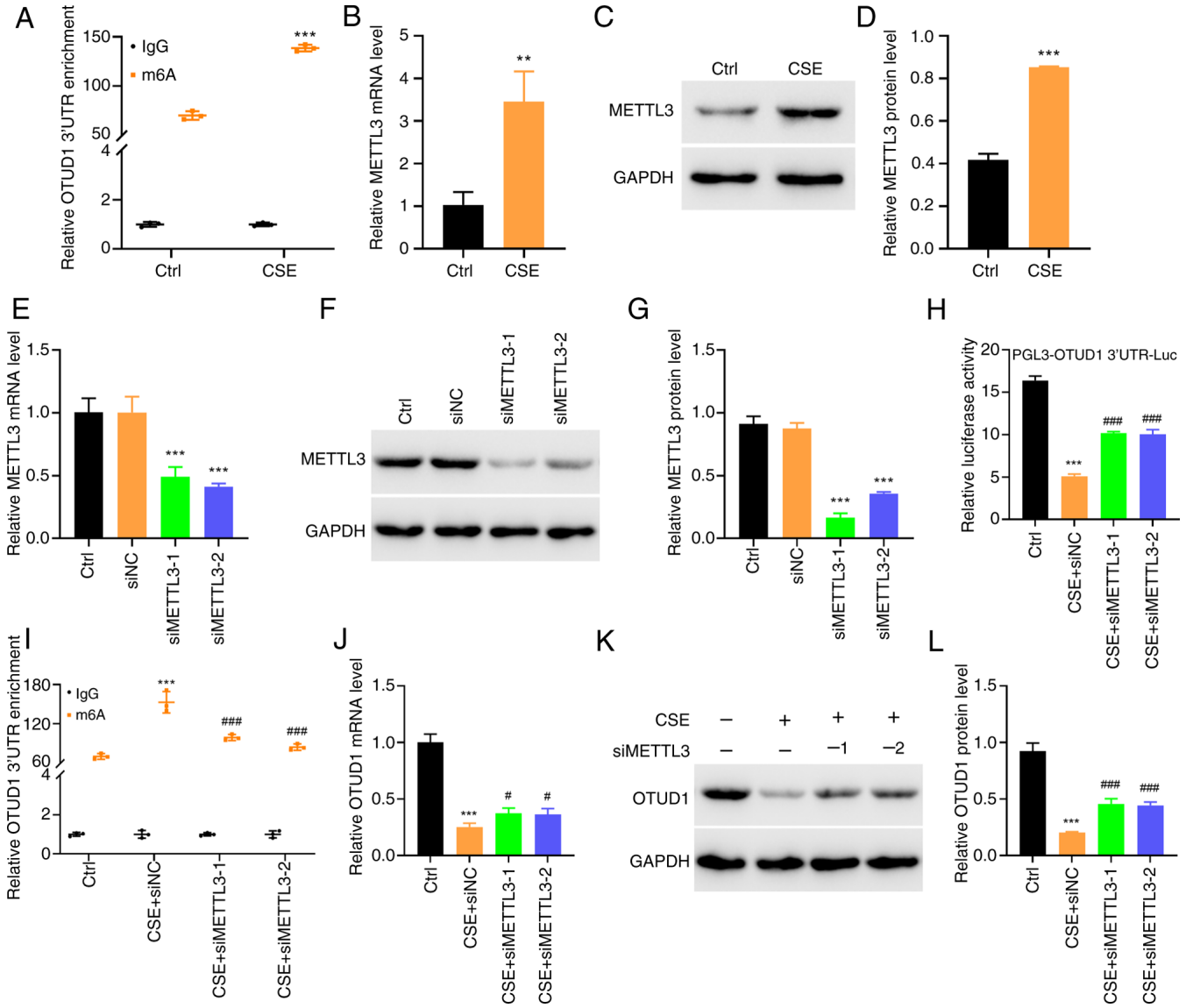

Figure 4. CSE induces METTL3 expression, promoting methylation of the OTUD1 3'UTR and inhibiting OTUD1 expression. (A) After treatment of BEAS-2B cells with 10% CSE for 24 h, the methylation level of the OTUD1 3'UTR was detected using meRIP-qPCR. ***P<0.001 vs. Ctrl. (B) RT-qPCR and (C) western blotting were used to detect changes in METTL3 mRNA and protein expression in cells. (D) Semi-quantitative analysis of METTL3 protein expression. BEAS-2B cells were transfected with siMETTL3 for 24 h, and changes in METTL3 mRNA and protein expression were detected by (E) RT-qPCR and (F) western blotting. (G) Semi-quantitative analysis of METTL3 protein expression. ***P<0.001 vs. siNC. (H) BEAS-2B cells were transfected with the pGL3-OTUD1 3'UTR luciferase reporter plasmid and siMETTL3, followed by treatment with 10% CSE for 24 h, and OTUD1 transcriptional activity was detected using a luciferase assay. (I) BEAS-2B cells were transfected with siMETTL3 and treated with 10% CSE for 24 h, and meRIP-qPCR was used to detect the methylation level of the OTUD1 3'UTR. (J) RT-qPCR and (K) western blotting were used to detect changes in OTUD1 mRNA and protein expression in cells. (L) Semi-quantitative analysis of OTUD1 protein expression. **P<0.01, ***P<0.001 vs. Ctrl; #P<0.05, ###P<0.001 vs. CSE + siNC. CSE, cigarette smoke extract; m6A, N6-methyladenosine; meRIP-qPCR, methylated RNA immunoprecipitation-quantitative PCR; METTL3, methyltransferase-like 3; NC, negative control; OTUD1, ovarian tumor protease domain-containing protein 1; RT-qPCR, reverse transcription-quantitative PCR; si, small interfering.

were constructed and cells were also treated with the NF-κB inhibitor PDTC. The results showed that siOTUD1 aggravated cell pyroptosis, increased the levels of the pro-inflammatory cytokines IL-1β and IL-18, and enhanced the expression levels of NF-κB and inflammasome-related proteins. However, the addition of PDTC, an NF-κB inhibitor, reduced the levels of pyroptosis and inflammation. These findings further confirm that OTUD1 may reduce cell damage induced by CSE by inhibiting inflammatory responses.

METTL3 and m6A are frequently dysregulated in various pathological processes, controlling the expression of specific genes and regulating cellular functions (36-38). Additionally, METTL3 and m6A are actively involved in the pathogenesis of pulmonary diseases, including chronic conditions such as pulmonary fibrosis, pulmonary arterial hypertension and COPD, as well as acute diseases such as pneumonia, SARS-CoV-2 infection and sepsis-induced acute respiratory distress syndrome (39,40). The RNA m6A modification mediated by METTL3 represents a novel mechanism underlying the onset and progression of these pulmonary diseases. Related research has indicated that METTL3 expression is notably increased in patients with smoking-induced COPD and COPD cell models (41,42). Furthermore, METTL3 silencing has been reported to inhibit the EMT process induced by CSE in human

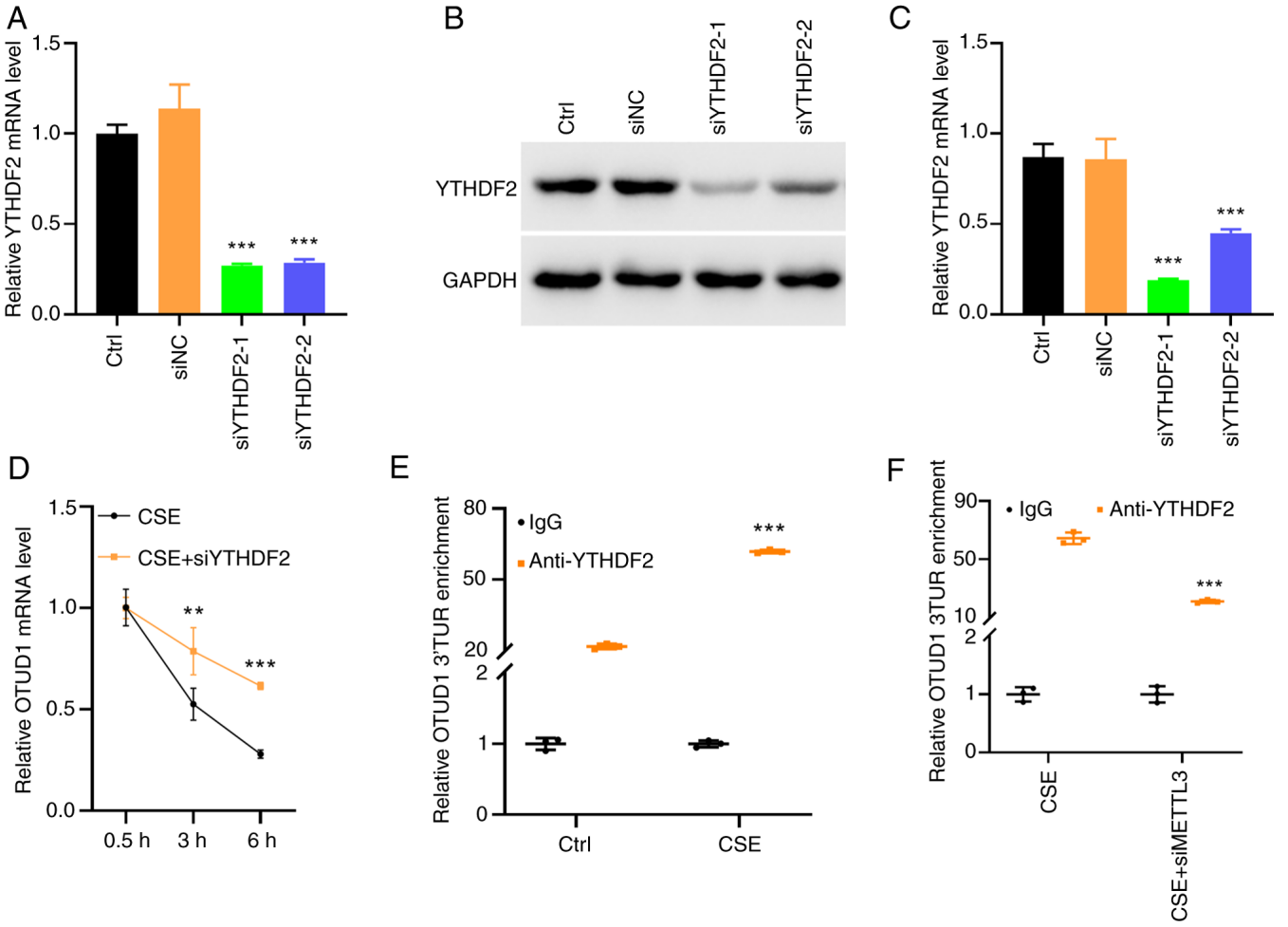

Figure 5. YTHDF2 regulates OTUD1 transcription. After transfecting BEAS-2B cells with siYTHDF2 for 24 h, changes in YTHDF2 mRNA and protein expression levels were detected by (A) RT-qPCR, (B) western blotting. (C) Smei-quantitative analysis of YTHDF2 protein expression. ***P<0.001 vs. siNC. siYTHDF2-1 was used for subsequent experiments. (D) After transfection of BEAS-2B cells with siYTHDF2, cells were treated with 10% CSE and 5 μg/ml actinomycin D for 0, 3 and 6 h, and collected for RT-qPCR to detect changes in OTUD1 mRNA expression. **P<0.01, ***P<0.001 vs. CSE. (E) BEAS-2B cells were treated with 10% CSE for 24 h, and the RIP assay was used to detect the enrichment of YTHDF2 on the OTUD1 3'UTR. ***P<0.001 vs. Ctrl. (F) BEAS-2B cells were transfected with siMETTL3 and treated with 10% CSE for 24 h, followed by RIP assay to detect YTHDF2 enrichment on OTUD1 3'UTR. ***P<0.001 vs. CSE. CSE, cigarette smoke extract; METTL3, methyltransferase-like 3; NC, negative control; OTUD1, ovarian tumor protease domain-containing protein 1; RIP, RNA immunoprecipitation; RT-qPCR, reverse transcription-quantitative PCR; si, small interfering; YTHDF2, YTH m6A RNA binding protein 2.

bronchial epithelial cells (BEAS-2B) (22). Mechanistically, METTL3 silencing reduced m6A methylation of OTUD1 mRNA in the current study, thereby enhancing OTUD1 protein expression. Bioinformatics analysis predicted the presence of m6A methylation sites in the 3'UTR of OTUD1. To explore the association between METTL3-mediated m6A methylation and OTUD1 expression, BEAS-2B cells were treated with 10% CSE, and RT-qPCR and western blotting were used to detect METTL3 expression. The results showed that METTL3 levels were increased following 10% CSE stimulation, leading to elevated m6A methylation of OTUD1 and reduced OTUD1 expression. Upon constructing siMETTL3 models, m6A methylation levels were decreased whereas OTUD1 expression was increased, suggesting that 10% CSE stimulation promotes m6A methylation via increased METTL3 expression, thereby inhibiting OTUD1 expression. Subsequently, interference models were constructed for the m6A methylation reader YTHDF2. Following cigarette smoke exposure, siYTHDF2 knockdown alleviated the decrease in OTUD1 expression caused by cigarette smoke. These findings suggested that cigarette smoke exposure may inhibit OTUD1 expression by promoting m6A methylation, a process that requires the catalytic activity of METTL3 and the involvement of the reader YTHDF2. Cigarette smoke also increased the binding of YTHDF2 to the 3'UTR of OTUD1, which was partially suppressed by METTL3 knockdown. In conclusion, cigarette smoke exposure could increase the m6A methylation of OTUD1 involving METTL3 and YTHDF2, thereby inhibiting OTUD1 expression.

While previous studies have suggested that OTUD1 has tumor-suppressive properties, often linked to its ability to increase apoptosis in cancer cells (43,44), the findings of the present study indicated that OTUD1 may reduce pyroptosis in the context of COPD. This apparent contradiction may arise from the differing biological contexts in which OTUD1 functions. In cancer, the inhibition of NF-κB and other inflammatory pathways by OTUD1 often results in increased apoptosis of tumor cells, which is beneficial for limiting tumor progression (45). However, in COPD, the role of OTUD1 may shift towards protecting healthy lung cells from excessive inflammatory responses, such as

pyroptosis, which is commonly induced by cigarette smoke exposure (46).

In the present study, oeOTUD1 reduced pyroptosis in BEAS-2B cells treated with CSE, suggesting that OTUD1 serves a protective role in the lungs under inflammatory stress conditions. This protective effect is likely due to its ability to inhibit excessive inflammation by suppressing NF-κB activation and inflammasome-related proteins, such as NLRP3 and GSDMD-N. Through this mechanism, OTUD1 may reduce cell damage and maintain cellular integrity, which contrasts with its pro-apoptotic effect in the context of cancer cells, where inflammation and immune evasion are significant factors. Further investigation into the specific mechanisms by which OTUD1 modulates inflammation and pyroptosis in different disease contexts will help to clarify its dual role in cellular responses.

In conclusion, in patients with COPD affected by cigarette smoke exposure, OTUD1 expression may decrease as the disease progresses. The OTUD1 gene reduces cell damage and inflammation caused by cigarette smoke exposure by inhibiting inflammatory responses. CSE (10%) was shown to inhibit OTUD1 expression by upregulating METTL3, which may enhance METTL3-mediated methylation and promote YTHDF2 recognition of OTUD1 methylation. Although the present study revealed the potential role of OTUD1 through database analysis and cellular experiments, these findings have not yet been validated in patient samples. Future research should use clinical data to analyze OTUD1 expression in tissue samples obtained from patients with COPD and to assess its association with disease severity, with the aim of enhancing the clinical applicability of these findings.

Acknowledgements

Not applicable.

Funding

The present study was supported by the Natural Science Foundation of China (grant no. 2023YFC3043507), Shanghai Pudong Hospital and the Discipline Construction Promoting Project of Shanghai Pudong Hospital (grant no. Zdzk2020-11).

Availability of data and materials

The data generated in the present study may be requested from the corresponding author.

Authors' contributions

JG, ZS, WT, ZW and YS designed the project. ZS, WT, JX, WC and ZC performed experiments, data analysis and interpretation. The manuscript was drafted by JG and YS. Study supervision was carried out by ZW and YS. ZW and YS confirm the authenticity of all the raw data. All authors read and approved the final version of the manuscript.

Ethics approval and consent to participate

Not applicable.

Patient consent for publication

Not applicable.

Competing interests

The authors declare that they have no competing interests.

References

1. Agustí A, Celli BR, Criner GJ, Halpin D, Anzueto A, Barnes P, Bourbeau J, Han MK, Martinez FJ, Montes de Oca M, *et al*: Global initiative for chronic obstructive lung disease 2023 report: GOLD executive summary. Eur Respir J 61: 2300239, 2023.
2. Brandsma CA, Van den Berge M, Hackett TL, Brusselle G and Timens W: Recent advances in chronic obstructive pulmonary disease pathogenesis: From disease mechanisms to precision medicine. J Pathol 250: 624-635, 2020.
3. Su X, Wu W, Zhu Z, Lin X and Zeng Y: The effects of epithelial-mesenchymal transitions in COPD induced by cigarette smoke: An update. Respir Res 23: 225, 2022.
4. GBD Chronic Respiratory Disease Collaborators: Prevalence and attributable health burden of chronic respiratory diseases, 1990-2017: A systematic analysis for the global burden of disease study 2017. Lancet Respir Med 8: 585-596, 2020.
5. Madawala S, Quach A, Lim JY, Varatharaj S, Perera B, Osadnik C and Barton C: Healthcare experience of adults with COPD during the COVID-19 pandemic: A rapid review of international literature. BMJ Open Respir Res 10: e001514, 2023.
6. Rabbani G, Shariful Islam SM, Rahman MA, Amin N, Marzan B, Robin RC and Alif SM: Pre-existing COPD is associated with an increased risk of mortality and severity in COVID-19: A rapid systematic review and meta-analysis. Expert Rev Respir Med 15: 705-716, 2021.
7. GBD 2017 Risk Factor Collaborators: Global, regional, and national comparative risk assessment of 84 behavioural, environmental and occupational, and metabolic risks or clusters of risks for 195 countries and territories, 1990-2017: A systematic analysis for the global burden of disease study 2017. Lancet 392: 1923-1994, 2018.
8. GBD 2019 Tobacco Collaborators: Spatial, temporal, and demographic patterns in prevalence of smoking tobacco use and attributable disease burden in 204 countries and territories, 1990-2019: A systematic analysis from the global burden of disease study 2019. Lancet 397: 2337-2360, 2021.
9. Niu Y, Niu H, Meng X, Zhu Y, Ren X, He R, Wu H, Yu T, Zhang Y, Kan H, *et al*: Associations between air pollution and the onset of acute exacerbations of COPD: A time-stratified case-crossover study in China. Chest 166: 998-1009, 2024.
10. Pathak U, Gupta NC and Suri JC: Risk of COPD due to indoor air pollution from biomass cooking fuel: A systematic review and meta-analysis. Int J Environ Health Res 30: 75-88, 2020.
11. Xing Z, Yang T, Shi S, Meng X, Chai D, Liu W, Tong Y, Wang Y, Ma Y, Pan M, *et al*: Combined effect of ozone and household air pollution on COPD in people aged less than 50 years old. Thorax 79: 35-42, 2023.
12. Lamichhane DK, Leem JH and Kim HC: Associations between ambient particulate matter and nitrogen dioxide and chronic obstructive pulmonary diseases in adults and effect modification by demographic and lifestyle factors. Int J Environ Res Public Health 15: 363, 2018.
13. Shakeel I, Ashraf A, Afzal M, Sohal SS, Islam A, Kazim SN and Hassan MI: The molecular blueprint for chronic obstructive pulmonary disease (COPD): A new paradigm for diagnosis and therapeutics. Oxid Med Cell Longev 2023: 2297559, 2023.
14. Ming T, Liu H, Yuan M, Tian J, Fang Q, Liu Y, Kong Q, Wang Q, Song X, Xia Z and Wu X: The deubiquitinase OTUD1 deubiquitinates TIPE2 and plays a protective role in sepsis-induced lung injury by targeting TAK1-mediated MAPK and NF-κB signaling. Biochem Pharmacol 227: 116418, 2024.
15. Ma X, Wang L, Shi G and Sun S: The deubiquitinase OTUD1 inhibits non-small cell lung cancer progression by deubiquitinating and stabilizing KLF4. Thorac Cancer 13: 761-770, 2022.
16. Zhang Q, Li J, Chen Z, Jiang K, Yang K, Huang F, Huang A, Zhang X, Zhang J and Wang H: VE-822 upregulates the deubiquitinase OTUD1 to stabilize FHL1 to inhibit the progression of lung adenocarcinoma. Cell Oncol (Dordr) 46: 1001-1014, 2023.

17. Wu B, Qiang L, Zhang Y, Fu Y, Zhao M, Lei Z, Lu Z, Wei YG, Dai H, Ge Y, *et al*: The deubiquitinase OTUD1 inhibits colonic inflammation by suppressing RIPK1-mediated NF-κB signaling. Cell Mol Immunol 19: 276-289, 2022.
18. Zheng S, Li Y, Song X, Wu M, Yu L, Huang G, Liu T, Zhang L, Shang M, Zhu Q, *et al*: OTUD1 ameliorates cerebral ischemic injury through inhibiting inflammation by disrupting K63-linked deubiquitination of RIP2. J Neuroinflammation 20: 281, 2023.
19. Yang Y, Fei Y, Xu X, Yao J, Wang J, Liu C and Ding H: Shikonin attenuates cerebral ischemia/reperfusion injury via inhibiting NOD2/RIP2/NF-κB-mediated microglia polarization and neuroinflammation. J Stroke Cerebrovasc Dis 33: 107689, 2024.
20. Zhong R, Wen C, Qiu Y, Shen X, Sun Z, Peng L, Liu T, Huang S and Peng X: Anti-inflammatory and immunomodulatory effects of Glycyrrhiza uralensis fisch. On ulcerative colitis in rats: Role of nucleotide-binding oligomerization domain 2/receptor-interacting protein 2/nuclear factor-kappa B signaling pathway. J Ethnopharmacol 344: 119457, 2025.
21. Zhang C, Chen L, Peng D, Jiang A, He Y, Zeng Y, Xie C, Zhou H, Luo X, Liu H, *et al*: METTL3 and N6-methyladenosine promote homologous recombination-mediated repair of DSBs by modulating DNA-RNA hybrid accumulation. Mol Cell 79: 425-442.e7, 2020.
22. Zhang Y, Wang L, Yan F, Yang M, Gao H and Zeng Y: Mettl3 mediated m6A methylation involved in epithelial-mesenchymal transition by targeting SOCS3/STAT3/SNAI1 in cigarette smoking-induced COPD. Int J Chron Obstruct Pulmon Dis 18: 1007-1017, 2023.
23. Song L, Liu H, Yang W, Yin H, Wang J, Guo M and Yang Z: Biological functions of the m6A reader YTHDF2 and its role in central nervous system disorders. Biochem Pharmacol 230: 116576, 2024.
24. Gao L, Lv G, Liu Z, Tian Y, Han F, Li L, Wang G and Zhang Y: Alcohol-induced C/EBP β-driven VIRMA decreases oxidative stress and promotes pancreatic ductal adenocarcinoma growth and metastasis via the m6A/YTHDF2/SLC43A2 pathway. Oncogene 44: 1118-1132, 2025.
25. Shuai Y, Ma Z, Ju J, Li C, Bai X, Yue J, Wang X, Yuan P and Qian H: The N6-methyladenosine writer METTL3 promotes breast cancer progression through YTHDF2-dependent posttranscriptional silencing of GSDMD. Apoptosis 30: 226-238, 2025.
26. Cau SBA, Guimaraes DA, Rizzi E, Ceron CS, Souza LL, Tirapelli CR, Gerlach RF and Tanus-Santos JE: Pyrrolidine dithiocarbamate down-regulates vascular matrix metalloproteinases and ameliorates vascular dysfunction and remodelling in renovascular hypertension. Br J Pharmacol 164: 372-381, 2011.
27. Livak KJ and Schmittgen TD: Analysis of relative gene expression data using real-time quantitative PCR and the 2(-Delta Delta C(T)) method. Methods 25: 402-408, 2001.
28. Ezzie ME, Crawford M, Cho JH, Orellana R, Zhang S, Gelinas R, Batte K, Yu L, Nuovo G, Galas D, *et al*: Gene expression networks in COPD: microRNA and mRNA regulation. Thorax 67: 122-131, 2012.
29. Faner R, Cruz T, Casserras T, López-Giraldo A, Noell G, Coca I, Tal-Singer R, Miller B, Rodriguez-Roisin R, Spira A, *et al*: Network analysis of lung transcriptomics reveals a distinct B-cell signature in emphysema. Am J Respir Crit Care Med 193: 1242-1253, 2016.
30. Xia H, Wu Y, Zhao J, Cheng C, Lin J, Yang Y, Lu L, Xiang Q, Bian T and Liu Q: N6-Methyladenosine-modified circSAV1 triggers ferroptosis in COPD through recruiting YTHDF1 to facilitate the translation of IREB2. Cell Death Differ 30: 1293-1304, 2023.
31. Huang K, Sun X, Xu X, Lu J, Zhang B, Li Q, Wang C, Ding S, Huang X, Liu X, *et al*: METTL3-mediated m6A modification of OTUD1 aggravates press overload induced myocardial hypertrophy by deubiquitinating PGAM5. Int J Biol Sci 20: 4908-4921, 2024.
32. Jing H, Song J, Sun J, Su S, Hu J, Zhang H, Bi Y and Wu B: METTL3 governs thymocyte development and thymic involution by regulating ferroptosis. Nat Aging 4: 1813-1827, 2024.
33. Chen J, Wang T, Li X, Gao L, Wang K, Cheng M, Zeng Z, Chen L, Shen Y and Wen F: DNA of neutrophil extracellular traps promote NF-κB-dependent autoimmunity via cGAS/TLR9 in chronic obstructive pulmonary disease. Signal Transduct Target Ther 9: 163, 2024.
34. Oikawa D, Gi M, Kosako H, Shimizu K, Takahashi H, Shiota M, Hosomi S, Komakura K, Wanibuchi H, Tsuruta D, *et al*: OTUD1 deubiquitinase regulates NF-κB- and KEAP1-mediated inflammatory responses and reactive oxygen species-associated cell death pathways. Cell Death Dis 13: 694, 2022.
35. Oikawa D, Shimizu K and Tokunaga F: Pleiotropic roles of a KEAP1-associated deubiquitinase, OTUD1. Antioxidants (Basel) 12: 350, 2023.
36. Liu Y, Yang D, Liu T, Chen J, Yu J and Yi P: N6-methyladenosine-mediated gene regulation and therapeutic implications. Trends Mol Med 29: 454-467, 2023.
37. Su X, Lu R, Qu Y and Mu D: Diagnostic and therapeutic potentials of methyltransferase-like 3 in liver diseases. Biomed Pharmacother 172: 116157, 2024.
38. Su X, Lu R, Qu Y and Mu D: Methyltransferase-like 3 mediated RNA m^6 A modifications in the reproductive system: Potentials for diagnosis and therapy. J Cell Mol Med 28: e18128, 2024.
39. Ledford H: How air pollution causes lung cancer-without harming DNA. Nature 616: 419-420, 2023.
40. Su X, Feng Y, Qu Y and Mu D: Association between methyltransferase-like 3 and non-small cell lung cancer: Pathogenesis, therapeutic resistance, and clinical applications. Transl Lung Cancer Res 13: 1121-1136, 2024.
41. Wang Q, Shen J, Luo S, Yuan Z, Wei S, Li Q, Yang Q, Luo Y and Zhuang L: METTL3-m6A methylation inhibits the proliferation and viability of type II alveolar epithelial cells in acute lung injury by enhancing the stability and translation efficiency of Pten mRNA. Respir Res 25: 276, 2024.
42. Ambrosino P, Vitacca M, Marcuccio G, Spanevello A, Ambrosino N and Maniscalco M: A comparison of GOLD and STAR severity stages in individuals with COPD undergoing pulmonary rehabilitation. Chest 167: 387-401, 2025.
43. Zhang Z, Fan Y, Xie F, Zhou H, Jin K, Shao L, Shi W, Fang P, Yang B, van Dam H, *et al*: Breast cancer metastasis suppressor OTUD1 deubiquitinates SMAD7. Nat Commun 8: 2116, 2017.
44. Liu H, Zhong L, Lu Y, Liu X, Wei J, Ding Y, Huang H, Nie Q and Liao X: Deubiquitylase OTUD1 confers Erlotinib sensitivity in non-small cell lung cancer through inhibition of nuclear translocation of YAP1. Cell Death Discov 8: 403, 2022.
45. Zhou T, Wu Y, Qian D, Tang H, Liu X, Qiu J, Wang D, Hong W, Meng X and Zheng Q: OTUD1 chemosensitizes triple-negative breast cancer to doxorubicin by modulating P16 expression. Pathol Res Pract 247: 154571, 2023.
46. Xie W, Luo B and Zhang L: Effect of AMPK on the apoptosis in NHBE cells of COPD induced by CSE. China J Mod Med 24: 28-33, 2014.